frontiers in Earth Science

ORIGINAL RESEARCH
published: 23 November 2020
doi: 10.3389/feart.2020.604807

The Footprint of Atlantic Multidecadal Oscillation on the Intensity of Tropical Cyclones Over the Western North Pacific

Cheng Sun[1], Yusen Liu[1], Zhanqiu Gong[1], Fred Kucharski[2], Jianping Li[3,4], Qiuyun Wang[5] and Xiang Li[6]*

[1]College of Global Change and Earth System Science (GCESS), Beijing Normal University, Beijing, China, [2]The Abdus Salam International Centre for Theoretical Physics, Trieste, Italy, [3]Frontiers Science Center for Deep Ocean Multispheres and Earth System (FDOMES), Key Laboratory of Physical Oceanography, Institute for Advanced Ocean Studies, Ocean University of China, Qingdao, China, [4]Laboratory for Ocean Dynamics and Climate, Pilot National Laboratory for Marine Science and Technology (Qingdao), Qingdao, China, [5]Key Laboratory of Mesoscale Severe Weather/Ministry of Education and School of Atmospheric Sciences, Nanjing University, Nanjing, China, [6]Key Laboratory of Marine Hazards Forecasting, National Marine Environmental Forecasting Center, Ministry of Natural Resources, Beijing, China

Sea surface temperature (SST) over the western North Pacific (WNP) exhibits strong decadal to multidecadal variability and in this region, warm waters fuel the tropical cyclones (TCs). Observational records show pronounced decadal variations in WNP TC metrics during 1950–2018. Statistical analysis of the various TC metrics suggests that the annual average intensity of WNP TCs is closely linked to the AMO ($r = 0.86$ at decadal timescales, $p < 0.05$). Observations and coupled atmosphere-ocean simulations show that the decadal WNP SST variations regarded as the primary driver of TC intensity, are remotely controlled by the AMO. Corresponding to the WNP SST warming, the local SLP gets lower and the tropospheric air becomes warmer and moister, enhancing atmospheric instability and the generation of convective available potential energy. These favorable changes in the background environment provide more "fuel" to the development of deep convection and intensify the WNP TCs. The footprints of AMO in WNP SST and atmospheric states through trans-basin interaction eventually exert a significant impact on the TC intensity over the WNP region.

Keywords: Atlantic multidecadal oscillation, inter-basin interaction, teleconnection, extreme weather and climate, tropical cyclone

OPEN ACCESS

Edited by:
Wei Zhang,
The University of Iowa, United States

Reviewed by:
Si Gao,
Sun Yat-sen University, China
Chao Wang,
Nanjing University of Information Science and Technology, China

****Correspondence:***
Cheng Sun
scheng@bnu.edu.cn

Specialty section:
This article was submitted to Atmospheric Science, a section of the journal Frontiers in Earth Science

Received: *10 September 2020*
Accepted: *28 October 2020*
Published: *23 November 2020*

Citation:
Sun C, Liu Y, Gong Z, Kucharski F, Li J, Wang Q and Li X (2020) The Footprint of Atlantic Multidecadal Oscillation on the Intensity of Tropical Cyclones Over the Western North Pacific. Front. Earth Sci. 8:604807. doi: 10.3389/feart.2020.604807

INTRODUCTION

Tropical cyclone (TC) is one of the most destructive natural disasters. Almost 30% of all TCs over the globe take place in the western North Pacific (WNP; 100°–180°E, 0°–40°N). As the surface temperature has warmed notably, observed changes in the WNP TC activity during the recent decades are metric dependent, showing a strengthening trend in the intensity but decreasing trends in the frequency and duration (Emanuel, 2005; Liu and Chan, 2013). In addition to the effects of climate change (Knutson et al., 2019; Knutson et al., 2020), internal climate variability can also influence TC activity. For example, WNP TC activity shows pronounced interannual variability and most studies have identified ENSO as an important contributor to the interannual variations (Chan 1985; Camargo and Sobel 2005; Wang et al., 2014; Liu and Chen 2018; Patricola et al., 2018).

Madden-Julian oscillation (MJO), Pacific–Japan (PJ) teleconnection and other atmospheric variabilities also play roles in influencing the WNP TC activity (Nakazawa 1986; Maloney and Hartmann 2001; Li et al., 2014; Wu et al., 2020; Zhou et al., 2019). Some other studies highlighted the remote effects of SST variability in Indian and Atlantic Oceans on WNP TCs but mostly focused on the frequency and genesis of TCs (Liu and Chan, 2008; Liu and Chan, 2013; Huo et al., 2015; Zhang et al., 2017; Gao et al., 2018; Zhang et al., 2018; Zhang and Villarini, 2019; Gao et al., 2020). Besides the interannual variability, some studies have suggested a significant multidecadal change in the WNP TC activity (Leung et al., 2005; Chan, 2006; Li and Zhou, 2014; Wang et al., 2015). However, there have been much fewer studies focusing on the decadal variations (or fluctuations) of the WNP TC activity, and the decadal variability of WNP TC intensity and the driving mechanism remain unclear.

It is widely recognized that sea surface temperature (SST) is an important environmental condition for TC activity (Gray and Brody, 1967; Landsea, 2005). The global SSTs show pronounced interdecadal variabilities and one of the most well-known patterns is the Atlantic Multidecadal Oscillation (AMO) (Kerr, 2000). Previous studies indicated that the AMO plays a crucial role in climate around the Atlantic region (Enfield et al., 2001; McCabe et al., 2004; Sutton and Hodson, 2005; Wang and Lee, 2009; Sutton and Dong, 2012), together with the remote regions (Lu et al., 2006; Li and Bates, 2007; Sun et al., 2015; Sun et al., 2017b). Hurricane activity over the North Atlantic basin has been linked to the AMO (Zhang and Delworth, 2007), indicating the effects of local SST variability. Meanwhile, inter-basin SST interactions at decadal time scales have received considerable attention in recent years as many studies have suggested a strong SST teleconnection from North Atlantic to Pacific (Li and Zhou, 2014; McGregor et al., 2014; Lopez et al., 2016; Ruprich-Robert et al., 2017). Particularly, some previous studies based on both modeling and observational analysis have suggested that the multidecadal variations in the SST and atmospheric circulation aloft over the western tropical Pacific and North Pacific are significantly influenced by the AMO signal (Sun et al., 2017a; Gong et al., 2020). Zhang et al. (2018) have linked the multidecadal variations of WNP TC genesis frequency since 1980 to the AMO, but the potential influence of AMO on the WNP TC intensity remains to be studied. Previous studies have reported that there are decadal variations in the WNP basin-wide TC intensity, showing an increasing trend since the mid-1970s (Wu et al., 2008; Wu and Zhao, 2012). Thus, it is of interest to examine the relationship between the AMO and TC intensity at decadal timescales.

Our analysis will focus on the decadal variations of the WNP TC activity. In this study, the accumulated cyclone energy (ACE) proposed by Bell et al. (2001) is used to represent the activity of TCs. In addition to the ACE index, the number of TCs (frequency), TC days, and average intensity are defined to distinguish the characteristics of TC activity. Detailed information can be found in the Methods. We also perform statistical analysis on a suite of Atlantic Pacemaker experiments to investigate the AMO effects on the WNP TC activity, and a strong connection at decadal time scales can be found. A mechanism is then proposed to explain the teleconnection between the AMO and WNP TC activity which connects the WNP climate to the North Atlantic Ocean. Our results highlight the remote influence of AMO on WNP TC activity. This may also have implications for better understanding the decadal variability and predictability of the WNP TC activity.

DATA AND METHODOLOGY

Data

The global observational SST data set used in this study is the Extended Reconstruction SST version 3 (ERSST v3b) data set (Smith et al., 2008). The atmospheric data set derives from the NOAA ESRL 20th Century Reanalysis, version 2 (20CRv2) (Compo et al., 2011) which includes air temperature, specific humidity and sea level pressure (SLP).

The data sets of the WNP TC metrics (the number of Named TCs, the Named TC days, and the Accumulated Cyclone Energy) we used are available online from the Department of Atmospheric Science at Colorado State University (http://tropical.atmos.colostate.edu/Realtime/). And the statistics are calculated from National Hurricane Center, the Central Pacific Hurricane Center and the Joint Typhoon Warning Center best tracks as archived in the International Best Track Archive for Climate Stewardship (IBTrACS) (Knapp et al., 2010; Knapp et al., 2018). The code for calculating the maximum potential intensity is publicly available (ftp://texmex.mit.edu/pub/emanuel/TCMAX/).

The AMO index is defined as the area-weighted average of SST anomalies over the North Atlantic region (0°–60°N, 80°W–0°). And the index used in this study comes from the NOAA ESRL Climate Timeseries, which is calculated from the Kaplan SST dataset (Enfield et al., 2001). Other indices of climate modes are obtained from the following websites: NPGO index: http://www.o3d.org/npgo/, IPO index: https://psl.noaa.gov/data/timeseries/IPOTPI/ and PDO index: https://cmdp.ncc-cma.net/pred/cn_enso.php?product=cn_enso_pdo.

Statistics of Western North Pacific Tropical Cyclone Activity

The Accumulated Cyclone Energy (ACE) index is a well-known statistic that uses the maximum wind speed over time to quantify cyclone activity (Bell, 2001). It is proposed to describe the total TC activity (Waple et al., 2002) and is calculated by integrating the squares of the maximum sustained surface wind every 6 h for named cyclones (greater than 34 knots).

$$\sum_{n=1}^{N} \int_{0}^{D(n)} V_{\max}^{2}(n,t)dt = \mathrm{ACE} \tag{1}$$

where the $V_{\max}$ is the maximum sustained surface wind. As shown in **Eq. 1**, for a specific year the ACE of WNP TCs equals the sum of the square of maximum sustained wind of TCs ($V_{\max}$) over all named TCs (denoted as N in the **Eq. 1**) and the corresponding TC durations (denoted as D in the **Eq. 1**). This

definition takes three key factors into account: the TC count, intensity, and duration of all the TCs in the active season of a year and indicates that the annual ACE is the numerical integral of a time series.

According to **Eq. 1**, ACE is a function of the TC intensity, duration and total count, describing the annual TC activity in a basin. To distinguish the individual contributions from the TC intensity, duration and total count to the annual TC activity from the ACE, Wu et al., (2008) defined a parameter of the annual average intensity of TCs for a specific basin. Following the method, the average intensity of WNP TCs for a specific year (denoted as V_a in the **Eq. 2**) is obtained by averaging the *V*max over the duration of each TC and then for all of the TCs in that year.

$$\sum_{n=1}^{N} \int_{0}^{D(n)} V_{\max}(n,t)dt = V_a \cdot \sum_{n=1}^{N} D(n) \quad (2)$$

Therefore, in addition to the parameter of annual ACE index, the annual TC activity in the WNP basin can be characterized by the TC average intensity and the annual accumulated TC duration (total TC days, $\sum_{n=1}^{N} D(n)$ in **Eq. 2**), and the latter can be further decomposed into TC total count and average duration (Wu et al., 2008; Zhao et al., 2011; Wu and Zhao, 2012).

Statistical Methods

We use a two-tailed Student's t-test to determine the statistical significance of the linear regression and correlation between two autocorrelated time series. The effective number of degrees of freedom is N^{eff}, which is given by the following approximation:

$$\frac{1}{N^{eff}} = \frac{1}{N} + \frac{2}{N}\sum_{j=1}^{N} \frac{N-j}{N} \rho_{XX}(j)\rho_{YY}(j)$$

where N is the sample size, and $\rho_{XX}(j)$ and $\rho_{YY}(j)$ are the autocorrelations of two sampled time series X and Y, respectively, at time lag j (Li et al., 2013; Sun et al., 2015).

Model and Experiments

We use the International Center for Theoretical Physics AGCM (ICTPAGCM, version 41) (Kucharski et al., 2016) developed from the general circulation model (GCM) with a coupled slab ocean thermodynamic mixed-layer model to perform an Atlantic Pacemaker experiment (partially coupled experiment, referred to as ATL_VARMIX). The code of ICTPAGCM is available through the URL: https://www.ictp.it/research/esp/models/speedy.aspx. The mixed-layer model includes spatially varying annual mean mixed-layer depths (varying from 40 m in tropics to 60 m in the extra-tropics). To investigate the WNP SST and atmospheric circulation responses to the Atlantic SST forcing, the SSTs over the Atlantic basin (60°S–60°N, 70°W–10°E) are prescribed using the observational monthly-varying SSTs from the Hadley Center Sea Ice and Sea Surface Temperature (HadISST) data set (Rayner et al., 2003). In the Indo-Pacific basins, the ocean is allowed to integrate the atmospheric heat fluxes and to interact with the atmosphere. Thus, the simulated SSTs in the Indo-Pacific basins are interactively generated by coupling with the slab ocean. The simulated variations in atmospheric circulation are the responses to the combined effects of Atlantic SST forcing and atmosphere-ocean coupling out of the Atlantic region. The large-scale environmental conditions for WNP TC activity in ATL_VARMIX (e.g., MPI and VWS) are further calculated based on the simulation results of SST and atmospheric variables.

The simulations of the ATL_VARMIX experiment are integrated from 1872 to 2013 and an ensemble of five members is generated to reduce the uncertainties due to different initial conditions. The ensemble mean of the five integrations is analyzed and displayed in the figures unless stated otherwise. More details about the ATL_VARMIX simulations can be found in the **Supplementary Material**.

RESULTS

Western North Pacific Tropical Cyclone Average Intensity and Climate Modes

In order to better understand the characteristics of WNP TC time series at decadal time scales, in this study, we mainly focus on the decadal variations of the four annual mean TC metrics, including annual accumulated cyclone energy (ACE), number of TCs (or frequency), total TC days and average intensity between 1950 and 2018, which are calculated using Joint Typhoon Warning Center (JTWC) best track dataset. The detailed definitions of these quantities are given in the *Methods* section. The index of each TC metric in WNP manifests significant decadal variability and two peaks can be found in this time series (**Figure 1**). More specifically, the time series of the TC days index (**Figure 1C**) shows a similar variation to that of ACE (**Figure 1A**) which reaches its maximum in the mid-1990s and exhibits a decreasing trend in the following 15 years. However, the frequency index (**Figure 1B**) reaches its maximum in the mid-1960s, earlier than the ACE and TC days. Here, the average intensity of TCs is defined as the mean intensity of all named cyclones in a year, and the product of the average intensity and the total number of TC days in that year equals the annual ACE index (see *Statistics of Western North Pacific Tropical Cyclone Activity* for details). Moreover, decadal variability in TC average intensity over WNP (**Figure 1D**) is also evident and manifests a decadal trend for about 20 to 30 years. There are two turning signs appearing in the 1970s and around 2000s which resemble the AMO index (Kerr, 2000), further implying the potential linkage between them. More evidence will be discussed in the following sections.

Then, the comparison between the AMO index and annual mean average intensity further supports our speculations based on the consistency of their turning signs. The time series of the AMO index (**Figure 2**) has approximately 50–60 years variation, with changes of sign in reverse polarity in the 1920s, 1960s and around 2000s (Schlesinger and Ramankutty, 1994; Enfield et al., 2001), demonstrating that the AMO and WNP TC average intensity are closely connected and share a similar decadal fluctuation. This result indicates that the variation of WNP

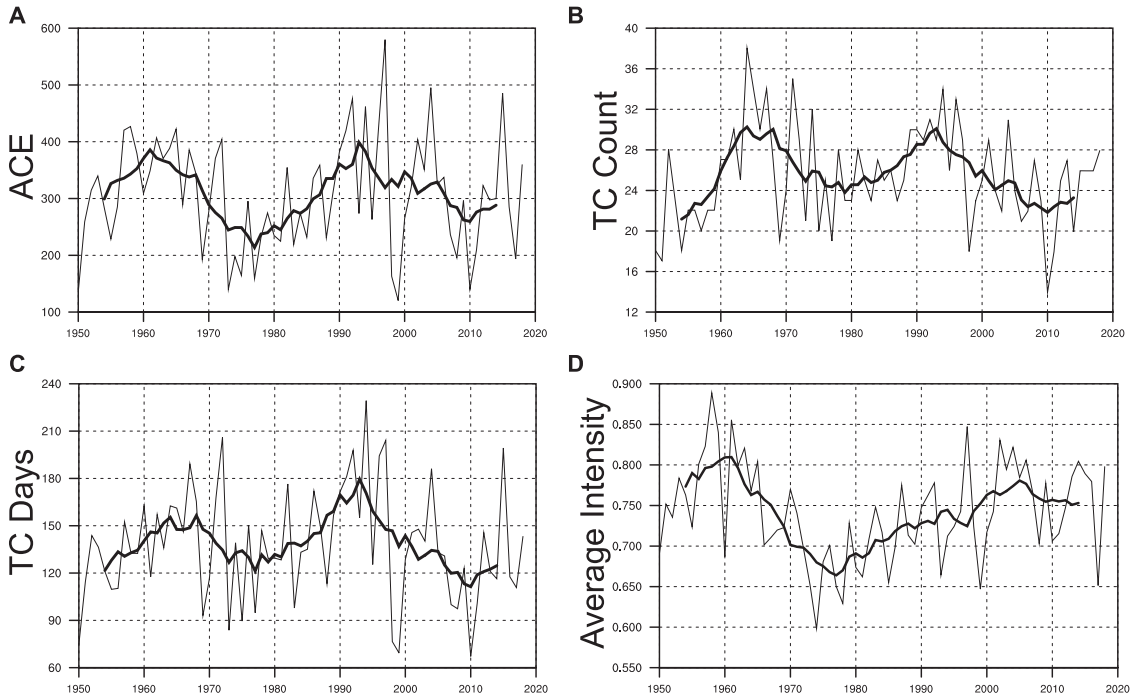

FIGURE 1 | Interannual-to-decadal variability of various TC metrics. Time series of annual mean **(A)** ACE index (unit: $10^4 \cdot knot^2$), **(B)** frequency, **(C)** TC days (unit: days) and **(D)** average intensity (unit: $10^2 \cdot knot$) of TCs in the western North Pacific as a function of time for 1950–2018 (thin solid black curve). The thick black curve in each panel shows the 9-year running averages. The long-term linear trends were removed.

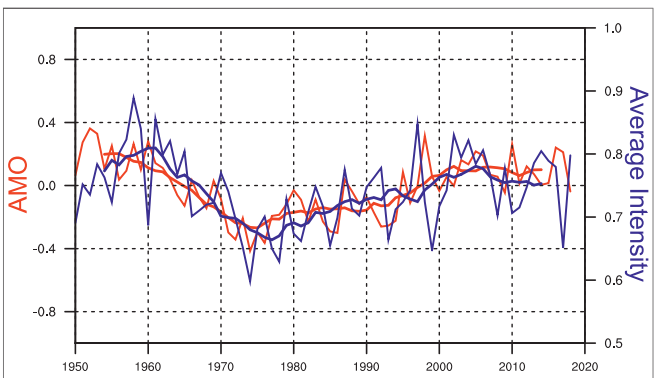

FIGURE 2 | Time series of annual mean average intensity (thin blue curve; unit: $10^2 \cdot knot$) and the AMO index (thin red curve; unit: K) for 1950–2018. The thick curves show the 9-year running averages. The long-term linear trends were removed.

TABLE 1 | Correlations Between Four WNP TC Metrics and AMO, PDO, IPO, and NPGO for 1950–2018.

Correlation coefficients	TC days	Frequency	ACE	Average intensity
AMO (1950–2018)	0.36 (13)	–0.35 (10)	0.36 (10)	**0.86** (4)
PDO (1950–2018)	**0.58** (11)	0.41 (9)	0.20 (7)	-0.29 (4)
IPO (1950–2018)	**0.65** (10)	0.46 (9)	0.24 (8)	-0.30 (5)
NPGO (1950–2018)	–**0.72** (12)	–**0.59** (11)	-0.43 (10)	0.10 (6)

The long-term linear trends were removed before analysis. Correlations significant at the 95% level based on the estimated effective degrees of freedom are underlined (in bold). The effective degrees of freedom are included in parentheses next to the correlation coefficient. The calculation of the effective degrees of freedom is given in the Methods.

TC average intensity is highly correlated to the remote AMO signal at decadal time scales and it might be affected by the North Atlantic basin.

As the Pacific Decadal Oscillation (PDO/IPO) (Mantua et al., 1997; Zhang et al., 1997) and North Pacific Gyre Oscillation (NPGO) have been recognized for playing a dominant role in modulating North Pacific SST at decadal time scales, it is essential to examine the correlations of Pacific SST variability with each of the four WNP TC metrics. Several studies have implied the possible effects of PDO, IPO and NPGO on WNP TC activity (Chan, 2008; Liu and Chan, 2008; Goh and Chan, 2010; Zhang et al., 2013). Thus, we further calculate the correlation coefficients between those four TC metrics and these decadal and multidecadal oceanic modes (the time series are shown in **Supplementary Figure S1** and the correlations are listed in **Table 1**), in order to clarify whether Pacific decadal SST variability has such correlations with WNP TC as AMO does and to highlight the relative roles of AMO and Pacific decadal SST variability on WNP TC activity. In general, the variations of the IPO and NPGO index are different from those of the AMO and the WNP TC average intensity, and the correlations of the TC intensity with the IPO and NPGO are low and insignificant. Nevertheless, the NPGO show significant

correlations with the WNP TC days and genesis frequency. This is consistent with the previous study which suggests a significant impact of NPGO on TC frequency. Meanwhile, the PDO/IPO might correlate to the total TC days but the correlation coefficient is relatively small. Such findings are consistent with the previous studies which indicated that the PDO plays a minor role in the decadal variations of WNP TC characteristics (i.e., frequency and intensity) and it can barely explain the regional-scale features of WNP climate variability (Zhang et al., 2013; Sun et al., 2017a; Gong et al., 2020). Another interesting thing is that the correlation coefficient between WNP TC average intensity and the AMO index reaches 0.86 ($p < 0.05$), further confirming the strong connection between them as is inferred from **Figure 2**. We can then conclude that the linkage between AMO and WNP TC intensity is robust at decadal time scales, while other TC metrics such as ACE, frequency and TC days show weaker correlations with the AMO.

Previous studies have suggested that the TC intensity records may be less reliable before the mid-1970s (Dvorak 1975; Chu et al., 2002; Ackerman et al., 2018). We repeat the above analysis but for a more recent period 1975–2018. As shown in **Supplementary Table S1**, the average intensity of WNP TCs is mostly correlated with the AMO for 1975–2018, while the effects of other SST modes are relatively insignificant. This is in good agreement with the results for the longer analysis period 1950–2018. The decadal-scale variation in average intensity during 1975–2018 is characterized by an increasing trend before 2000 and a flattening trend afterward. These variations are best matched with the AMO variability, leading to a highly positive correlation ($r = 0.89$, significant at the 95% confidence level). For the WNP TC days and frequency, the effects of Pacific SST modes (PDO, IPO, and NPGO) are stronger, with strong positive correlations observed for the PDO/IPO and negative correlations for the NPGO during 1975–2018. Similar negative correlations are also observed for the AMO, which shows a general warming trend during 1975–2018, coincident with the decreasing trend in the TC days and frequency. Zhang et al. (2018) have also suggested that the warming trend in AMO may lead to the decreasing of WNP TC frequency during the period 1980–2014. Nevertheless, consistent with the results for the longer period, the correlation of the AMO with the TC average intensity (0.89) is higher than that with the TC days and frequency (−0.71 and −0.68, respectively), indicating a more profound influence of AMO on the WNP TC intensity. **Supplementary Figure S2** further shows the correlation map between WNP TC average intensity and Northern Hemisphere SST at decadal timescales for the period 1975–2018. The SST correlations over the North Atlantic show a basin-wide coherent pattern with significant positive values that resembles the AMO. Therefore, both the analyses of temporal variations and the spatial pattern of SST correlations confirm the close relationship between the AMO and WNP TC average intensity for the more recent period 1975–2018, indicating that the finding of AMO footprint in WNP TC average intensity is insensitive to the analysis period.

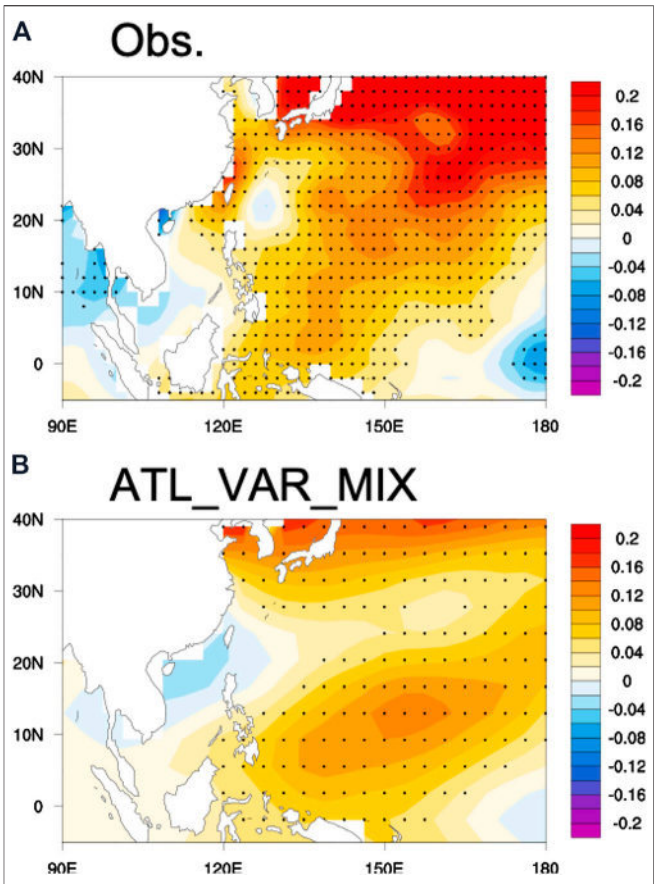

FIGURE 3 | (A) The regression map of SST anomalies (unit: K) onto the normalized AMO index based on the data from the ERSST data for 1950–2010. **(B)** As in **(A)**, but in the ATL_VARMIX experiment. The long-term linear trends in the SST data set were removed before the regression analysis, and dots indicate the regression coefficients significant at the 95% confidence level.

Western North Pacific Tropical Cyclone Average Intensity and TC Activity

The average intensity of TCs over the WNP basin is a basin-wide metric, and it is necessary to examine the relationships between this basin-wide metric and variations in TC characteristics (i.e., genesis location and track distributions). Observed TC data are obtained from the International Best Track Archive for Climate Stewardship (IBTrACS) including the Joint Typhoon Warning Center (JTWC), Japan Meteorological Agency (JMA), and Chinese Meteorological Administration (CMA) best track data. **Supplementary Figure S3** shows the regression map of the annual genesis density of WNP TCs on the basin-wide average intensity. The genesis density is calculated by counting the number of tropical cyclones with genesis (first position) in each 2.5° × 2.5° latitude and longitude square (Camargo et al., 2007). The regression map shows that the increase (decrease) of

the TC average intensity corresponds to more TC genesis over the western WNP basin and less TC genesis over the eastern WNP basin. The results based on the data sets from the three agencies are similar. We also analyze the relationship between average TC intensity and track distributions. The time series of WNP TC average intensity shows a period of weak intensity during 1970–1990 and two periods of strong intensity during 1950–1964 and 1996–2015. As shown in **Supplementary Figure S4**, the average TC genesis location during the strong intensity period (1950–1964 and 1996–2015) is to the west of that during the weak intensity period (1970–1990). This is consistent with the results of TC genesis density shown in **Supplementary Figure S3**. For the average TC track distributions, the TCs during the strong intensity period show a more north-oriented track compared with the weak intensity period, and the average TC track during the strong intensity period extends farther northward than the weak intensity period. Therefore, during the high TC intensity period, the TCs in the WNP basin tend to travel a relatively long distance. In addition, the intensity-related variations in TC genesis locations and track distributions for the TC active season (JJASO, **Supplementary Figure S5**) are generally consistent with the annual ones (**Supplementary Figures S3**, **S4**). Overall, the increase of WNP average TC intensity is associated with the westward shift of the TC genesis locations and the more northward extension of TC tracks.

Previous studies (Byers, 1944; Palmen, 1948; Malkus and Riehl, 1960; Chan et al., 2001) have illustrated the fundamental physical basis between TC average intensity and the ocean boundary and confirmed that the warm SST is favorable to the intensification of TCs over the Northern Hemisphere Oceans. Here, regression analyses are used to quantify the relationships between those factors associated with TC intensity and AMO index and to reveal the underlying mechanism. The regression map of 9-year running mean observational SST anomalies onto the normalized AMO index (**Figure 3A**) exhibits significant positive SST anomalies over the most area of the WNP region despite a slight northward shift of the maximum. The warm SST anomalies are strong and statistically significant over the western WNP basin, while over the eastern WNP, the SST anomalies are relatively weak and nearly opposite to the western WNP. We further calculate the latitudinal average of SST anomalies between the equator and 20°N (**Supplementary Figure S6**), which also shows a peak of warm SST anomalies between 110°E and 150°E, and east of 150°E, the SST anomalies decrease rapidly and become weak. This feature of WNP SST anomalies may explain the changes in the average genesis location of TCs revealed in the above analysis, and hence the average intensity of TCs formed in the WNP basin.

We can further infer that the AMO indeed affects WNP TC through modifying SST at decadal time scales, but the causality cannot be suggested only by statistical analysis. We then perform model simulations to further verify the remote effects of AMO on the WNP SST. Similar results can be found in the ATL_VARMIX experiment (Atlantic Pacemaker experiment, see *Methods*). The simulated regression pattern of WNP SST onto the AMO index is consistent with the observed one, and the regression coefficients are significant over the WNP region. Overall, the experiment does indicate the existence of warming responses of WNP SST to the AMO and the results are consistent with previous studies that explain the underlying mechanism of such phenomenon (Sun et al., 2017a; Gong et al., 2020; Wu et al., 2020). The warm AMO phase could induce anomalous surface high pressures over the northern and eastern Pacific which generate diverging flow toward the WNP, leading to anomalous convergence and low pressures there. The warm SST anomaly further develops due to the SST–sea level pressure–cloud–longwave radiation positive feedback. For the TC active season (June to October, JJASO), both observations and ATL_VARMIX simulations suggest a significant inter-basin SST teleconnection from North Atlantic to the WNP (**Supplementary Figure S7**), consistent with the annual mean data (**Figure 3**). The AMO-induced atmospheric teleconnection pattern is also similar to that based on annual mean data, showing anomalous high pressures in the northern and eastern Pacific accompanied by diverging flow toward the WNP. The WNP is dominated by anomalous convergence and low-pressure anomaly (**Supplementary Figure S7**), and the warm SST anomaly can be further developed and maintained through the local air-sea interaction. We can infer that the AMO may influence WNP TC average intensity by modifying SSTs in association with the inter-basin teleconnection. As shown in **Figure 3B**, the model shows the capability to reproduce the strong warm SST anomalies over the western WNP and rather weak SST anomalies in the eastern WNP, and the simulated latitudinal average of SST anomalies between the equator and 20°N also shows a peak of warm SST anomalies over the western WNP basin. It should be also noted that there is a discrepancy of SST anomaly center between observations and model simulations, indicating that the model experiment shows limitations in simulating the centers of maximum SST anomalies in the WNP associated with the AMO. Nevertheless, the model experiment reasonably reproduces the basin-wide SST warming in the WNP in response to the warm AMO phase, and the main structure of the observed SST anomaly pattern in the tropical WNP and the amplitude are fairly well reproduced by the model.

The effects of local SST changes on the WNP TC intensity at decadal timescales have also been highlighted in the previous studies (Wu and Zhao, 2012; Mei et al., 2015). Wu and Zhao (2012) compared the individual contributions of changes in local SST, vertical wind shear, and prevailing tracks to the increasing trend in WNP TC intensity over the period 1975–2007. They found that while the individual changes in vertical shear and prevailing tracks played an insignificant role in TC intensity, the warming SST over the period 1975–2007 significantly contributed to the multidecadal increasing trend in TC intensity. This is consistent with our present study that we also find the TC average intensity in WNP is closely related to the local SST at decadal timescales, and the increasing trend of TC average intensity is coincident with the SST warming during the period 1975–2018 (**Supplementary Figure S2**).

The relationship between local SST and TC intensity may be timescale dependent. The interannual component of TC average intensity is shown in **Supplementary Figure S8** by using a 2–9-

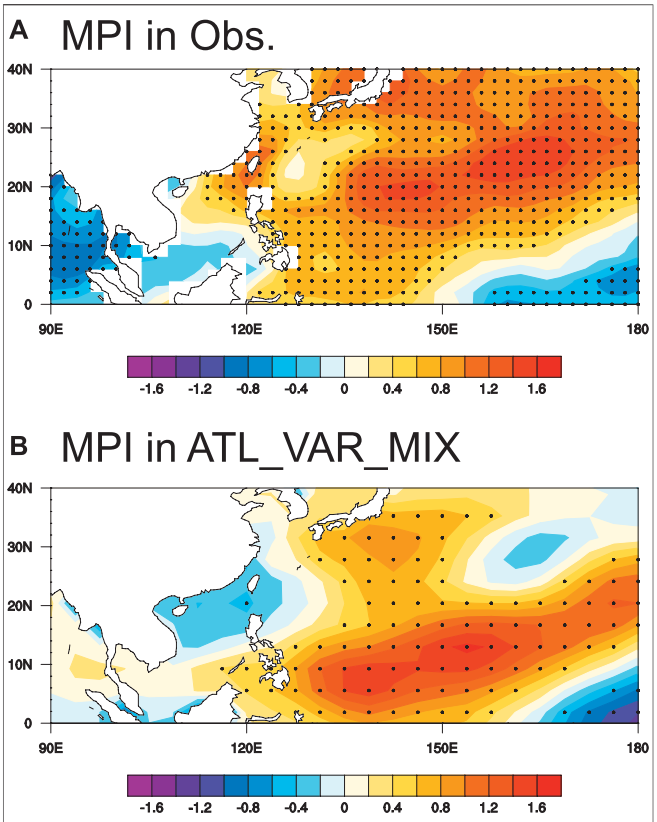

FIGURE 4 | The regression map of maximum potential intensity anomalies (m/s) onto the normalized AMO index based on the observational SST and 20CR atmospheric data for 1950–2010. **(B)** As in **(A)**, but in the ATL_VARMIX experiment. The long-term linear trends in the data were removed before the regression analysis, and dots indicate the regression coefficients significant at the 95% confidence level.

year band-pass filter. The correlation map of SST with interannual TC intensity is further shown in **Supplementary Figure S8**. The SST correlations clearly indicate an ENSO-like pattern, with positive correlations over the tropical central and eastern Pacific while negative correlations over the WNP region. This suggests that the ENSO significantly influences the WNP TC intensity at interannual timescales as previous studies suggested (Zhao et al., 2011). On the other hand, the negative SST correlations in WNP indicate that the dynamical large-scale parameters may play a more important role than the WNP local SST in the linkage between ENSO and WNP TC intensity (Zhao et al., 2011).

Roles of Large-Scale Environmental Factors

Relationships between the AMO index and other factors influencing WNP TC intensity are also examined. The moist convection associated with those factors plays a dominant role in the development of TCs and their average intensity (Raymond and Sessions, 2007). The maximum potential intensity is a direct quantity to represent the effects of large-scale environmental conditions on the TC intensity. Using the maximum potential intensity (MPI) theory (Bister and Emanuel 2002; Emanuel 2018), the estimated TC MPI anomalies in the WNP basin related to the AMO are shown in **Figure 4A**. The anomaly pattern suggests that the AMO-induced changes in SST and atmospheric conditions could result in significant variations in the MPI of TCs over the WNP, namely, the warm (cold) AMO phase could cause an overall significant increase (decrease) in the TC MPI. Particularly, at the lower latitudes (south of 10°N), the MPI anomaly pattern shows significant positive anomalies over the western WNP, and in the eastern WNP, the anomalies are relatively weak and nearly of opposite sign. This pattern of the MPI is consistent with the SST anomalies, further suggesting a key role of SST anomalies in modulating, the intensity of TCs in WNP. In this study, the MPI is used as a proxy to represent the effects of large-scale environmental conditions on the TC intensity. At decadal timescales, the variability of WNP MPI is closely related to the TC average intensity, indicating a significant impact of large-scale environmental conditions over the WNP (**Supplementary Figure S9**). In **Figure 5B**, lower tropospheric air temperature over the WNP region exhibits a uniformly warming response to the AMO. The sea level pressure (SLP) field is first examined, and the regression between AMO and SLP (**Figure 5A**) shows prominent consistency with that in SST. The warming in the ocean surface related to the AMO would further decrease the sea surface pressure over the entire WNP region. Thus, it supports that the WNP SSTs interact with the AMO and favor more intense TCs to develop. Corresponding to the responses of WNP SST to the AMO, it could be induced by the ocean-atmosphere interaction, with more heat fluxes released from a warmer ocean surface. The pattern of air temperature over 300 hPa shows similar results, but more significant warming can be found over the WNP region. Despite the differences in distributions of maximum centers between upper and lower troposphere, it still indicates tropospheric warming in WNP associated with the AMO. As for specific humidity (**Figures 5C,D**), positive moisture anomalies are most pronounced in WNP, especially near the tropics. Unlike the air temperature, the lower-level specific humidity shows more significantly increased responses to the AMO than the upper level, which is probably due to more water vapor content at the lower level and thus is more sensitive to the temperature changes.

By calculating the regressions of each factor onto the AMO index, potential linkages between them can be addressed as follow. All the variables exhibit significant responses to the AMO. In the WNP region, the SST warming induced by the AMO would reduce the sea surface pressure and increase the low-level air temperature, further intensifying the ascending motion and increasing the water vapor content. As a result, more water vapor could be pumped into the upper troposphere and release the latent heat above the lifting condensation level (LCL), heating the air over upper levels. Previous studies have pointed out that the increased low-level specific humidity and warm air temperature anomalies would intensify convective activity, such as TC (Gettelman et al., 2002; Chen et al., 2019). Low-level specific humidity can intensify positive buoyancy and more latent heat release, and in this case, the decrease in SLP provides

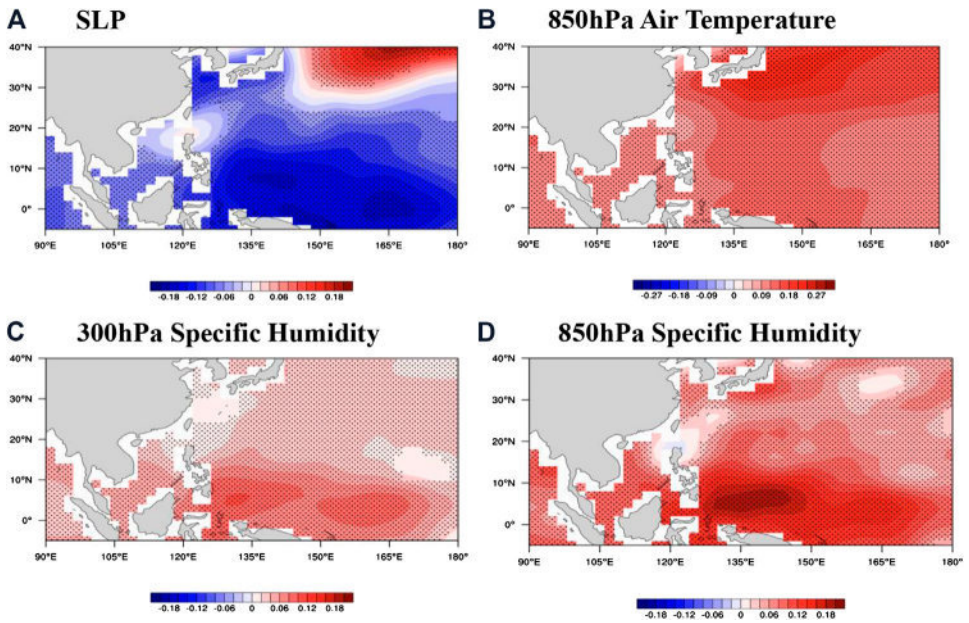

FIGURE 5 | The regression maps of **(A)** sea level pressure (unit: hPa), **(B)** 850 hPa air temperature anomalies (unit: K), **(C)** 300 hPa specific humidity anomalies (unit: $g \cdot kg^{-1}$), and **(D)** 850 hPa specific humidity anomalies (unit: $g \cdot kg^{-1}$) onto the normalized AMO index for 1950–2010 in 20CR reanalysis data. Dotted shading in **(A–D)** represents the regression coefficients significant at the 95% confidence level. The long-term linear trends for 1950–2010 in all variables were removed before the regression analysis.

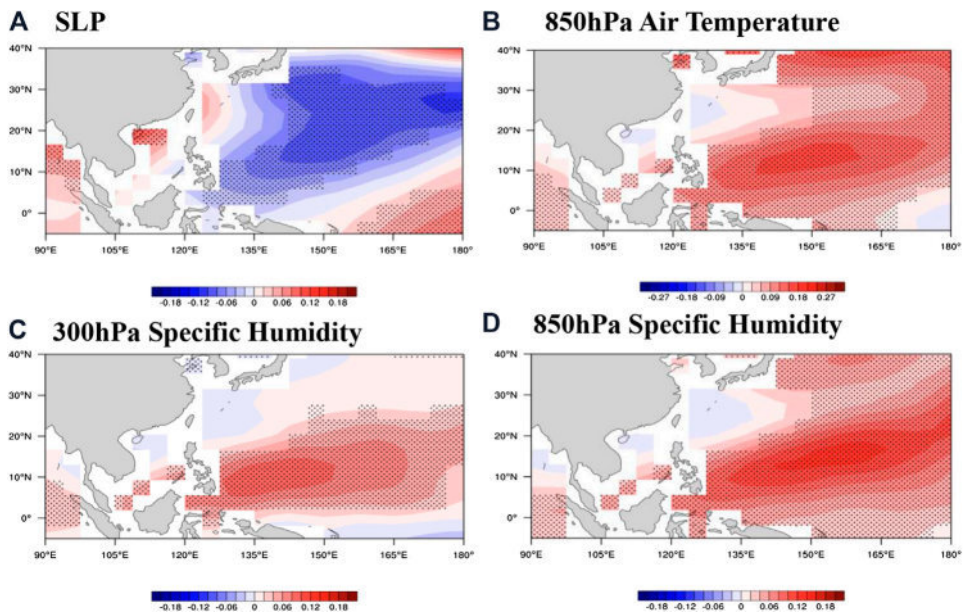

FIGURE 6 | The regression maps of **(A)** sea level pressure (unit: hPa), **(B)** 850 hPa air temperature anomalies (unit: K), **(C)** 300 hPa specific humidity anomalies (unit: $g \cdot kg^{-1}$), and **(D)** 850 hPa specific humidity anomalies (unit: $g \cdot kg^{-1}$) onto the normalized AMO index for 1950–2010 in the ATL_VARMIX experiment. Dotted shading represents the regression coefficients significant at the 95% confidence level. The long-term linear trends were removed.

favorable initial perturbation for the air parcel being easily lifted and passes the level of free condensation (LFC) to derive convective energy from the atmosphere and be able to ascend automatically. The WNP convective available potential energy (CAPE) anomalies in response to the remote AMO SST forcing correspond to the local SST warming and exhibit significantly

increased responses over most of the WNP region (**Supplementary Figure S10**). Thus, more CAPE will be produced with more latent heat released, and stronger warming and moistening at the lower level further amplifies this effect. Previous studies have also pointed out that the increased low-level specific humidity and warm air temperature anomalies would contribute to more CAPE genesis, which plays an important role in the rapid intensification of the WNP TCs (Gao et al., 2017), and the enhanced CAPE further acts as a crucial bridge linking the WNP SST warming and increase TC intensity. Meanwhile, other variables, especially to air temperature and specific humidity which are favorable to the increased MPI, also exhibit physically consistent responses to the AMO. Based on the observation and the ATL_VARMIX simulations, we can so far conclude that WNP atmospheric variables are closely linked to the remote AMO and shows significantly increased responses.

Model simulation is then carried out to highlight the role of AMO in the anomalies of atmospheric variables related to the WNP TC intensity, and the same calculations performed in **Figure 4A** and **Figure 5** are also applied to the ATL_VARMIX experiment. The Atlantic pacemaker experiment (ATL_VARMIX) captures the main structure of the MPI anomalies in the observation (**Figure 4B**), further indicating that the AMO signal could induce an overall increase/decrease in the MPI of TCs over the WNP. The SLP response to the AMO (**Figure 6A**) is similar to that in the observation, as the decrease in SLP induced by the AMO can be seen in the WNP region. In addition, the distribution of significant regression coefficients, corresponding to the SST warming, shows prominent consistency with the observation. It should be noted that the physical connections between MPI and other variables (SLP, air temperature and water vapor) are well captured by the model, as the variables in WNP show consistent anomalies in response to the North Atlantic SST forcing. Nevertheless, the vertical structure of air temperature in response to the AMO exhibits different quantitative relationships between the upper and lower level. In the ATL_VARMIX, the lower-level air temperature shows stronger warming responses to the AMO, compared with the upper level. The simulated distribution of the maximum responses of 850 hPa air temperature to the AMO (**Figure 6B**) is located over the WNP region, which is consistent with the simulated SST anomalies as more heat is released from a warmer ocean surface (**Figure 3B**). The distributions of upper-level and low-level specific humidity anomalies under the AMO forcing (**Figures 6C,D**) are similar to the observational results (**Figure 5C and 5D**). In the ATL_VARMIX experiment, WNP atmospheric factors exhibit significant responses to the AMO, which is also consistent with the observation. This result provides model evidence for the conclusion emphasized above, that both troposphere air warming and moistening are favorable for the TC average intensity under the AMO forcing in the WNP region.

Given the significant relationships between AMO, MPI and those associated factors have been discussed above (the correlation maps are also shown in Supplementary Material), how do they influence the TC intensity and connect it to the remote AMO? First of all, SST has long been recognized as the primary factor that modifies the TC intensity. Model evidence suggests that when other environmental factors are fixed, the varied SST still contributes to the variations in TC intensity. In the WNP region, strong responses can be found in local SST to the AMO forcing (Sun et al., 2017a; Wu et al., 2020). The warmed SST related to the AMO would lower the minimum central pressure around the core and provide favorable backgrounds, such as large-scale convergence and SLP decrease for the ascending motion (**Figures 5A**, **6A**). Thus, more energy can be released from the ocean to the atmosphere and directly contributes to the intensification of TC activities. In addition, SST warming would increase the water vapor content and enhance the moist instability over the lower troposphere (**Figures 5D**, **6D**). As mentioned above, the WNP SST warming induced by the AMO through the inter-basin SST teleconnection (Sun et al., 2017a; Gong et al., 2020) can partially explain such correlation between WNP TC intensity and the AMO. Moreover, WNP SST warming also induces significant changes in the vertical stability of the atmospheric column that may regulate the development of TCs. The TC intensity is closely linked to the ascending motion in the eyewall that the air parcel must extract energy from the ocean

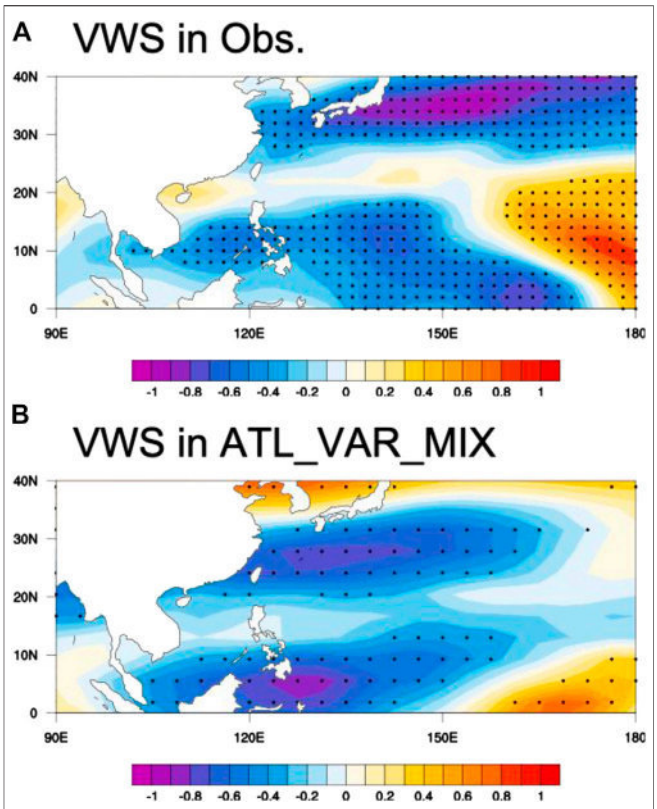

FIGURE 7 | The regression map of vertical wind shear (wind differences between 850 hPa and 200 hPa levels, m/s) anomalies onto the normalized AMO index based on the data from the 20CRv2 for 1950–2010. **(B)** As in **(A)**, but in the ATL_VARMIX experiment. The long-term linear trends in the data were removed before the regression analysis, and dots indicate the regression coefficients significant at the 95% confidence level.

and atmosphere to fight against gravity for elevation. In association with the WNP SST warming, the local SLP decrease and tropospheric warming and moistening lead to the increase of MPI over the WNP region (**Figures 4A,B**) and hence provide a favorable environment for TC intensification. Therefore, the interaction between lower-boundary SST and atmospheric factors intensifies the deep convection and provides energy to drive the development of TCs. Based on that, the strong connection between AMO and WNP TC intensity can be explained by the inter-basin footprints of AMO on the WNP SST and the associated atmospheric states.

We finally investigate the role of vertical wind shear (VWS) in the modulation of the WNP TC variations. The regression maps of WNP VWS anomalies on the AMO index are shown in **Figure 7**. In association with the warm AMO phase, the VWS anomalies over the WNP show an overall reduction over the WNP region, corresponding to the overall increase of average TC intensity. This suggests that the VWS indeed plays an important role in the connection between AMO and average TC intensity in the WNP. In addition, the zonal structure of the VWS at the lower latitudes shows a nearly dipole structure, with significantly reduced VWS over the western WNP and stronger VWS over the eastern WNP. The weakened-VWS region extends eastward to about 170°E, but the intensified-VWS region is limited to the east of 170°E. This pattern of VWS anomalies is consistent with the previous study (Zhang et al., 2018). The SST warming in WNP induces strong lower-level convergence, accompanied by lower-level westerly anomalies in the western WNP and easterly anomalies to the east (Sun et al., 2017a). Given the climatological easterlies in the lower levels over the WNP region, the intensified easterlies induce stronger VWS over the eastern WNP and westerly anomalies tend to weaken the VWS (Zhang et al., 2018), leading to the anomaly pattern of VWS shown in **Figure 7**. Moreover, the pattern of VWS is also consistent with the changes in genesis locations of WNP TCs, leading to the westward shift of TC genesis locations (Zhang et al., 2018). The overall reduction of WNP VWS and its spatial pattern are reproduced in the ATL_VARMIX simulations, providing further modeling evidence to support the influence of AMO on the WNP VWS, which could further affect the TC intensity.

SUMMARY AND DISCUSSION

In this study, we find a significant decadal variability of TC activity in the WNP region, based on the observational data set from 1950 to 2018. Statistical analysis of the various TC metrics suggests that the average intensity of WNP TCs is strongly connected with the AMO ($r = 0.86$ at decadal timescales, $p < 0.05$), showing a much closer relationship than other TC statistics (i.e., frequency and TC days). Observations and coupled atmosphere-ocean simulations show significant decadal SST warming over the WNP region in response to the AMO warm phase, which acts as a primary driver of the increase in TC intensity. The associated atmospheric changes also provide a favorable background environment. Corresponding to the SST warming, the local SLP decrease and the tropospheric air warming and moistening would enhance the atmospheric instability, which provides more energy to the development of deep convection and intensify the WNP TCs. In conclusion, the AMO-induced changes in SST and atmospheric states in WNP through trans-basin interaction eventually exert a significant impact on the TC intensity over the WNP region.

This study reveals a close relationship between AMO and WNP TC average intensity. The connections of AMO with other TC metrics, like the genesis frequency, are relatively weak. A possible explanation for this may lie in the distribution of the anomalous genesis density (**Supplementary Figure S3**). The genesis density anomaly pattern associated with the AMO indicates a westward/eastward shift of the WNP TC genesis rather than a basin-wide increase/decrease of the TC genesis over the entire WNP region. This anomalous pattern of WNP TC genesis density can be explained by the VWS anomalies (**Figure 7**). During the warm AMO phase, the VWS shows weakened VWS in the western WNP and intensified VWS in the eastern WNP, leading to the westward shift of TC genesis locations.

Our findings may help us better understand the impacts of AMO on the WNP climate, especially to the TC activity, which causes large damage to the adjacent countries. Thus, it could be a useful indicator for TC intensity prediction, when we take the North Atlantic signal into consideration. The main findings in the present study are based on the available records of WNP TC data since 1950, and future research is warranted as more observational records accumulate. Although the fundamental linkage between WNP TC intensity and the AMO can be reasonably well reproduced by the model, some biases can still be found, possibly due to the simplified and idealized physics of the coupled model. Thus, state-of-the-art coupled models with more comprehensive physics would be needed to better reproduce such mechanisms and reduce model uncertainties. The mixed layer ocean model shows the capability to reproduce the roles of SST and large-scale environment conditions in connecting the AMO to WNP TC intensity. Despite this, further modeling studies are required to understand the possible role of ocean dynamics in shaping the AMO-TC intensity linkage. A shortcoming of the simulations in the current study is low resolution, and TCs cannot be directly simulated by the model. Nevertheless, the main findings here indicate that statistical insights into the variations of TC metrics may be gained from these simulations.

DATA AVAILABILITY STATEMENT

The original contributions presented in the study are included in the article/**Supplementary Material**, further inquiries can be directed to the corresponding author.

AUTHOR CONTRIBUTIONS

CS designed the research. CS, ZG, and YL performed the data analysis, prepared all figures and led the writing of the

manuscript. All the authors discussed the results and commented on the manuscript.

FUNDING

This work was jointly supported by the National Natural Science Foundation of China (41775038, 41790474, and 41975082), National Key Research and Development Program of China (2016YFA0601801), and the National Program on Global Change and Air–Sea Interaction (GASI-IPOVAI-06 and GASI-IPOVAI-03).

SUPPLEMENTARY MATERIALS

The Supplementary Material for this article can be found online at: https://www.frontiersin.org/articles/10.3389/feart.2020.604807/full#supplementary-material

REFERENCES

Ackerman, S., Platnick, S., Bhartia, P., Duncan, B., L'ecuyer, T., Heidinger, A., et al. (2018). Satellites see the world's atmosphere. *Meteorol. Monogr.* 59, 4.1–4.53. doi:10.1175/AMSMONOGRAPHS-D-18-0009.1

Bell, W. (2001). Report 10. ESCAP Ii: estimation of correlation bias in 2000 ace estimates using revised demographic analysis results executive steering committee for ACE policy II.

Bister, M., and Emanuel, K. A. (2002). Low frequency variability of tropical cyclone potential intensity 1. Interannual to interdecadal variability. *J. Geophys. Res.: Atmosphere* 107 (D24), ACL 26-1–ACL 26-15. doi:10.1029/2001jd000776

Byers, H. R. (1944). "Atmospheric turbulence and the wind structure near the surface of the earth," in *General meteorology* (New York: McGraw-Hill Book Co., Inc.), ch. XXIV.

Camargo, S. J., and Sobel, A. H. (2005). Western North pacific tropical cyclone intensity and enso. *J. Clim.* 18 (15), 2996–3006. doi:10.1175/jcli4282.1

Camargo, S. J., Emanuel, K. A., and Sobel, A. H. (2007). Use of a genesis potential index to diagnose enso effects on tropical cyclone genesis. *J. Clim.* 20 (19), 4819–4834. doi:10.1175/jcli3457.1

Chan, J. C. L., Shi, J.-E., and Liu, K. S. (2001). Improvements in the seasonal forecasting of tropical cyclone activity over the western North pacific. *Weather Forecast.* 16 (4), 491–499. doi:10.6057/2012TCRR03.07

Chan, J. C. L. (1985). Tropical cyclone activity in the northwest pacific in relation to the el niño/southern oscillation phenomenon. *Mon. Weather Rev.* 113 (4), 599–606. doi:10.1175/1520-0493(1985)113<0599:TCAITN>2.0.CO;2

Chan, J. C. (2006). Comment on" changes in tropical cyclone number, duration, and intensity in a warming environment. *Science* 311 (5768), 1713. doi:10.1126/science.1121522

Chan, J. C. L. (2008). Decadal variations of intense typhoon occurrence in the western North pacific. *Proc. Math. Phys. Eng. Sci.* 464, 249–272.

Chen, X., Zhang, J. A., and Marks, F. D. (2019). A thermodynamic pathway leading to rapid intensification of tropical cyclones in shear. *Geophys. Res. Lett.* 46 (15), 9241–9251. doi:10.1029/2019gl083667

Chu, J.-H., Sampson, C. R., Levine, A. S., and Fukada, E. (2002). The joint typhoon warning center tropical cyclone best-tracks, 1945–2000. Ref. NRL/MR/7540-02 16

Compo, G. P., Whitaker, J. S., Sardeshmukh, P. D., Matsui, N., Allan, R. J., Yin, X., et al., (2011). The Twentieth Century reanalysis project. *Q. J. R. Meteorol. Soc.* 137 (654), 1–28. doi:10.1002/qj.776

Dvorak, V. F. (1975). Tropical cyclone intensity analysis and forecasting from satellite imagery. *Mon. Weather Rev.* 103, 420–430. doi:10.1175/1520-0493(1975)103<0420:TCIAAF>2.0.CO;2

Emanuel, K. (2005). Increasing destructiveness of tropical cyclones over the past 30 years. *Nature* 436 (7051), 686–688. doi:10.1038/nature03906

Emanuel, K. (2018). 100 years of progress in tropical cyclone research. *Meteorol. Monogr.* 59, 15.1–15.68. doi:10.1175/AMSMONOGRAPHS-D-18-0016.1

Enfield, D. B., Mestas-Nuñez, A. M., and Paul, J. T. (2001). The Atlantic multidecadal oscillation and its relation to rainfall and river flows in the continental us. *Geophys. Res. Lett.* 28 (10), 2077–2080. doi:10.1029/2000gl012745

Gao, S., Chen, Z., and Zhang, W. (2018). Impacts of tropical North Atlantic SST on western North Pacific landfalling tropical cyclones. *J. Clim.* 31, 853–862. doi:10.1175/jcli-d-17-0325.1

Gao, S., Chen, Z., Zhang, W., and Shen, X. (2020). Effects of tropical North Atlantic sea surface temperature on intense tropical cyclones landfalling in China. *Int. J. Climatol.* doi:10.1002/joc.6732

Gao, S., Zhai, S. N., Chen, B. Q., and Li, T. (2017). Water budget and intensity change of tropical cyclones over the western North pacific. *Mon. Weather Rev.* 145, 3009–3023. doi:10.1175/mwr-d-17-0033.1

Gettelman, A., Seidel, D. J., Wheeler, M. C., and Ross, R. J. (2002). Multidecadal trends in tropical convective available potential energy. *J. Geophys. Res. Atmosphere* 107 (D21), 4606. doi:10.1029/2001jd001082

Goh, A. Z.-C., and Chan, J. C. L. (2010). Interannual and interdecadal variations of tropical cyclone activity in the south China sea. *Int. J. Climatol.* 30 (6), 827–843. doi:10.1002/joc.1943

Gong, Z., Sun, C., Li, J., Feng, J., Xie, F., Ding, R., et al. (2020). An inter-basin teleconnection from the north Atlantic to the subarctic North Pacific at multidecadal time scales. *Clim. Dynam.* 54 (1-2), 807–822. doi:10.1007/s00382-019-05031-5

Gray, W. M., and Brody, L. (1967). Global view of the origin of tropical disturbances and storms: citeseer.

Huo, L., Guo, P., Hameed, S. N., and Jin, D. (2015). The role of tropical Atlantic sst anomalies in modulating western North pacific tropical cyclone genesis. *Geophys. Res. Lett.* 42 (7), 2378–2384. doi:10.1002/2015gl063184

Kerr, R. A. (2000). A North Atlantic climate pacemaker for the centuries. *Science* 288 (5473), 1984–1985. doi:10.1126/science.288.5473.1984

Knapp, K. R., Kruk, M. C., Levinson, D. H., Diamond, H. J., and Neumann, C. J. (2010). The international best track archive for climate stewardship (ibtracs) unifying tropical cyclone data. *Bull. Am. Meteorol. Soc.* 91 (3), 363–376. doi:10.1175/2009bams2755.1

Knapp, K. R., Velden, C. S., and Wimmers, A. J. (2018). A global climatology of tropical cyclone eyes. *Mon. Weather Rev.* 146 (7), 2089–2101. doi:10.1175/mwr-d-17-0343.1

Knutson, T, Camargo, S. J., Chan, J. C. L., Emanuel, K., Ho, C.-H., Kossin, J., et al. (2020). Tropical cyclones and climate change Assessment: Part II: projected response to Anthropogenic warming. *Bull. Am. Meteorol. Soc.* 101 (3), E303–E322. doi:10.1175/BAMS-D-18-0194.1

Knutson, T., Camargo, S. J., Johnny, C. L., Emanuel, K., Ho, C.-H., James, K., et al. (2019). Tropical cyclones and climate change Assessment: Part I: detection and attribution. *Bull. Am. Meteorol. Soc.* 100 (10), 1987–2007. doi:10.1175/BAMS-D-18-0189.1

Kucharski, F., Parvin, A., Rodriguez-Fonseca, B., Farneti, R., Martin-Rey, M., Polo, I., et al. (2016). The teleconnection of the tropical Atlantic to indo-pacific sea surface temperatures on inter-annual to centennial time scales: a review of recent findings. *Atmosphere* 7 (2), 29. doi:10.3390/atmos7020029

Landsea, C. W. (2005). Hurricanes and global warming. *Nature* 438 (7071), E11–E12. doi:10.1038/nature04477

Leung, Y. K., Wu, M. C., and Chang, W. L. (2005). Variations of tropical cyclone activity in the south China sea. *ESCAP/WMO Typhoon Committ. Ann. Rev.* 1, 277–292. doi:10.6057/2012TCRR02.01

Li, J., Sun, C., and Jin, F.-F. (2013). NAO implicated as a predictor of northern Hemisphere mean temperature multidecadal variability. *Geophys. Res. Lett.* 40 (20), 5497–5502. doi:10.1002/2013GL057877

Li, R. C. Y., and Zhou, W. (2014). Interdecadal change in south China sea tropical cyclone frequency in association with zonal sea surface temperature gradient. *J. Clim.* 27 (14), 5468–5480. doi:10.1175/jcli-d-13-00744.1

Li, R. C. Y., Zhou, W., and Li, T. (2014). Influences of the pacific–Japan teleconnection pattern on synoptic-scale variability in the western North pacific. *J. Clim.* 27 (1), 140–154. doi:10.1175/jcli-d-13-00183.1

Li, S., and Bates, G. T. (2007). Influence of the Atlantic multidecadal oscillation on the winter climate of east China. *Adv. Atmos. Sci.* 24 (1), 126–135. doi:10.1007/s00376-007-0126-6

Liu, K. S., and Chan, J. C. L. (2008). Interdecadal variability of western North pacific tropical cyclone tracks. *J. Clim.* 21 (17), 4464–4476. doi:10.1175/2008jcli2207.1

Liu, K. S., and Chan, J. C. L. (2013). Inactive period of western North pacific tropical cyclone activity in 1998–2011. *J. Clim.* 26 (8), 2614–2630. doi:10.1175/JCLI-D-12-00053.1

Liu, Y., and Chen, G. (2018). Intensified influence of the enso modoki on boreal summer tropical cyclone genesis over the western North pacific since the early 1990s. *Int. J. Climatol.* 38, e1258–e1265. doi:10.1002/joc.5347

Lopez, H., Dong, S., Lee, S.-K., and Goni, G. (2016). Decadal modulations of interhemispheric global atmospheric circulations and monsoons by the south Atlantic meridional overturning circulation. *J. Clim.* 29 (5), 1831–1851. doi:10.1175/JCLI-D-15-0491.1

Lu, R., Dong, B., and Ding, H. (2006). Impact of the Atlantic multidecadal oscillation on the Asian summer monsoon. *Geophys. Res. Lett.* 33 (24), L24701. doi:10.1029/2006gl027655.

Malkus, J. S., and Riehl, H. (1960). On the dynamics and energy transformations in steady-state hurricanes. *Tellus* 12 (1), 1–20. doi:10.1111/j.2153-3490.1960.tb01279.x

Maloney, E. D., and Hartmann, D. L. (2001). The madden–julian oscillation, barotropic dynamics, and North pacific tropical cyclone formation. Part I: observations. *J. Atmos. Sci.* 58 (17), 2545–2558. doi:10.1175/1520-0469(2001)058<2545:tmjobd>2.0.co;2

Mantua, N. J., Hare, S. R., Zhang, Y., Wallace, J. M., and Francis, R. C. (1997). A pacific interdecadal climate oscillation with impacts on salmon production. *Bull. Am. Meteorol. Soc.* 78 (6), 1069–1080. doi:10.1175/1520-0477(1997)078<1069:apicow>2.0.co;2

McCabe, G. J., Palecki, M. A., and Betancourt, J. L. (2004). Pacific and Atlantic Ocean influences on multidecadal drought frequency in the United States. *Proc. Natl. Acad. Sci. U.S.A.* 101 (12), 4136–4141. doi:10.1073/pnas.0306738101

McGregor, S., Timmermann, A., Stuecker, M. F., England, M. H., Merrifield, M., Jin, F.-F., et al. (2014). Recent walker circulation strengthening and pacific cooling amplified by Atlantic warming. *Nat. Clim. Change* 4 (10), 888–892. doi:10.1038/nclimate2330

Mei, W., Xie, S.-P., Primeau, F., Mcwilliams, J. C., and Pasquero, C. (2015). Northwestern Pacific typhoon intensity controlled by changes in ocean temperatures. *Sci. Adv.* 1, e1500014. doi:10.1126/sciadv.1500014

Nakazawa, T. (1986). Intraseasonal variations of olr in the tropics during the fgge year. *J. Meteorolog. Soc. Japan. Ser. II* 64 (1), 17–34. doi:10.2151/jmsj1965.64.1_17

Palmen, E. (1948). On the formation and structure of tropical hurricanes. *Geophysica* 3 (1), 26–38.

Patricola, C. M., Camargo, S. J., Klotzbach, P. J., Saravanan, R., and Chang, P. (2018). The influence of enso flavors on western North pacific tropical cyclone activity. *J. Clim.* 31 (14), 5395–5416. doi:10.1175/jcli-d-17-0678.1

Raymond, D. J., and Sessions, S. L. (2007). Evolution of convection during tropical cyclogenesis. *Geophys. Res. Lett.* 34 (6), L06811. doi:10.1029/2006gl028607

Rayner, N. A. A., Parker, D. E., Horton, E. B., Folland, C. K., Alexander, L. V., Rowell, D. P., et al. (2003). Global analyses of sea surface temperature, Sea Ice, and night marine air temperature since the late nineteenth Century. *J. Geophys. Res. Atmosphere* 108 (D14), 4407. doi:10.1029/2002JD002670

Ruprich-Robert, Y., Msadek, R., Castruccio, F., Yeager, S., Delworth, T., and Danabasoglu, G. (2017). Assessing the climate impacts of the observed Atlantic multidecadal variability using the gfdl Cm2. 1 and ncar Cesm1 global coupled models. *J. Clim.* 30 (8), 2785–2810. doi:10.1175/jcli-d-16-0127.1

Schlesinger, M. E., and Ramankutty, N. (1994). An oscillation in the global climate system of period 65–70 years. *Nature* 367 (6465), 723–726. doi:10.1038/367723a0

Smith, T. M., Reynolds, R. W., Peterson, T. C., and Lawrimore, J. (2008). Improvements to noaa's historical merged land–ocean surface temperature analysis (1880–2006). *J. Clim.* 21 (10), 2283–2296. doi:10.1175/2007jcli2100.1

Sun, C., Kucharski, F., Li, J., Jin, F.-F., Kang, I.-S., and Ding, R. (2017a). Western tropical pacific multidecadal variability forced by the Atlantic multidecadal oscillation. *Nat. Commun.* 8 (1), 1–10. doi:10.1038/ncomms15998

Sun, C., Li, J., Ding, R., and Jin, Z. (2017b). Cold season Africa–Asia multidecadal teleconnection pattern and its relation to the Atlantic multidecadal variability. *Clim. Dynam.* 48 (11-12), 3903–3918. doi:10.1007/s00382-016-3309-y

Sun, C., Li, J., and Zhao, S. (2015). Remote influence of Atlantic multidecadal variability on siberian warm season precipitation. *Sci. Rep.* 5, 16853. doi:10.1038/srep16853

Sutton, R. T., and Dong, B. (2012). Atlantic Ocean influence on a shift in European climate in the 1990s. *Nat. Geosci.* 5 (11), 788–792. doi:10.1038/ngeo1595

Sutton, R. T., and Hodson, D. L. R. (2005). Atlantic Ocean forcing of north American and European summer climate. *Science* 309 (5731), 115–118. doi:10.1126/science.1109496

Wang, C., and Lee, S. K. (2009). Co-variability of tropical cyclones in the North Atlantic and the eastern North Pacific. *Geophys. Res. Lett.* 36, L24702. doi:10.1029/2009gl041469

Wang, X., Wang, C., Zhang, L., and Wang, X. (2015). Multidecadal variability of tropical cyclone rapid intensification in the western North Pacific. *J. Clim.* 28, 3806–3820. doi:10.1175/jcli-d-14-00400.1

Wang, X., Zhou, W., Li, C., and Wang, D. (2014). Comparison of the impact of two types of El Niño on tropical cyclone genesis over the South China Sea. *Int. J. Climatol.* 34, 2651–2660. doi:10.1002/joc.3865

Waple, A. M., Lawrimore, J. H., Halpert, M. S., Bell, G. D., Higgins, W., Lyon, B., et al. (2002). Climate Assessment for 2001. *Bull. Am. Meteorol. Soc.* 83 (6), S1–S62. doi:10.1175/1520-0477(2002)083<0938:caf>2.3.co;2

Wu, L., Wang, B., and Braun, S. A. (2008). Implications of tropical cyclone power dissipation index. *Int. J. Climatol.* 28, 727–731. doi:10.1002/joc.1573

Wu, L., and Zhao, H. (2012). Dynamically derived tropical cyclone intensity changes over the western North Pacific. *J. Clim.* 25, 89–98. doi:10.1175/2011jcli4139.1

Wu, Q., Wang, X., and Tao, L. (2020). Interannual and interdecadal impact of western North pacific subtropical high on tropical cyclone activity. *Clim. Dynam.* 54 (3-4), 2237–2248. doi:10.1007/s00382-019-05110-7

Zhang, R., and Delworth, T. L. (2007). Impact of the Atlantic multidecadal oscillation on North Pacific climate variability. *Geophys. Res. Lett.* 34 (23), L23708. doi:10.1029/2007gl031601.

Zhang, W., Leung, Y., and Min, J. (2013). North Pacific gyre oscillation and the occurrence of western North pacific tropical cyclones. *Geophys. Res. Lett.* 40 (19), 5205–5211. doi:10.1002/grl.50955

Zhang, W., Vecchi, G. A., Murakami, H., Villarini, G., Delworth, T. L., Yang, X., et al. (2018). Dominant role of Atlantic multidecadal oscillation in the recent decadal changes in western North pacific tropical cyclone activity. *Geophys. Res. Lett.* 45 (1), 354–362. doi:10.1002/2017gl076397

Zhang, W., and Villarini, G. (2019). Seasonal forecasting of western North pacific tropical cyclone frequency using the north American multi-model ensemble. *Clim. Dynam.* 52 (9-10), 5985–5997. doi:10.1007/s00382-018-4490-y

Zhang, W., Vecchi, G. A., Villarini, G., Murakami, H., Rosati, A., Yang, X., et al. (2017). Modulation of western North pacific tropical cyclone activity by the Atlantic meridional mode. *Clim. Dynam.* 48 (1-2), 631–647. doi:10.1007/s00382-016-3099-2

Zhang, Y., Wallace, J. M., and Battisti, D. S. (1997). ENSO-Like interdecadal variability: 1900–93. *J. Clim.* 10 (5), 1004–1020. doi:10.1175/1520-0442(1997)010<1004:eliv>2.0.co;2

Zhao, H., Wu, L., and Zhou, W. (2011). Interannual changes of tropical cyclone intensity in the western North Pacific. *J. Meteorolog. Soc. Japan Ser. II* 89, 243–253. doi:10.2151/jmsj.2011-305

Zhou, Q., Wei, L., and Zhang, R. (2019). Influence of Indian ocean dipole on tropical cyclone activity over western North pacific in Boreal Autumn. *J. Ocean Univ. China* 18 (4), 795–802. doi:10.1007/s11802-019-3965-8

Conflict of Interest: The authors declare that the research was conducted in the absence of any commercial or financial relationships that could be construed as a potential conflict of interest.